

# EVOLUTION OF A MODULATED ELECTRON BEAM IN PLASMA FOR DIFFERENT MODES OF BEAM-PLASMA TURBULENCE

I.O. ANISIMOV, M.J. KIYANCHUK

UDC 533  
©2008

Taras Shevchenko Kyiv National University, Faculty of Radiophysics  
(6, Academician Glushkov Prosp., Kyiv 03127, Ukraine)

Evolution of a modulated electron beam in plasma for different beam-plasma turbulence modes is studied via a computer simulation using the PIC method. Ranges of the beam current density corresponding to different modes of beam-plasma turbulence were found out from the simulation. Peculiarities of the interference of non-resonant (at the modulation frequency) and resonant instabilities for different modes of beam-plasma turbulence are investigated. A modulation instability was observed in the strong turbulence mode. Quasiperiodic transillumination of the plasma by an electron beam is observed for the superstrong turbulence mode.

## 1. Introduction

Beam-plasma interaction has been studied during several decades (see, e.g., [1,2]), but this field still contains a lot of unresolved problems.

The problem of modulated electron beam's evolution in plasma is of interest in various branches of plasma electronics such as electron beams' using as the emitters of electromagnetic waves in ionosphere [3,4], inhomogeneous plasma diagnostics via the transition radiation of electron beams and electron bunches [5,6], transillumination of the dense plasma barriers for electromagnetic waves using electron beams [7], excitation of wake waves for high-gradient electrons' acceleration [8], *etc.*

Evolution of modulated electron beams in plasma was studied in [7, 9–12]. In these papers, the influence of a beam initial modulation depth on its evolution in supercritical plasma was investigated analytically, numerically, and experimentally. Experiment [9, 10] demonstrated that the signal at a modulation frequency reached its maximum inside the barrier, and magnitude of this maximum was directly proportional to the initial beam modulation depth. These results were explained in [11] by the concurrence between non-resonant (signal) and resonant (noise) modes of the beam-plasma system. But the results of calculations

presented in [11] correspond to the initial problem, whereas the results of experiments [9, 10] correspond to the boundary-value problem. As a result, it was impossible to compare experiments and the results of simulation.

In our previous work [12], the evolution of a modulated electron beam in plasma for the initial-boundary problem was studied via a computer simulation using the PIC method. It was shown that the concurrence of resonant and non-resonant mode leads to the suppression of the non-resonant mode, similarly to results in [11]. In contrast to the previous simulation [11], it was demonstrated that the resonant instability appears and develops in the wide frequency range, and its spectrum is continuous. All these results correspond to experimental data [9, 10].

During studying the spatial evolution of the electric field spectrum and the electron beam density spectrum in [12], it was found out that the behavior of a signal at the resonant frequency and the modulation frequency depended significantly on the electron beam current density which defines the mode of beam-plasma turbulence. So, this article is devoted to the study of the interference of a signal and resonant modes for weak, strong, and superstrong turbulence modes in the beam-plasma system.

## 2. Simulation Method and Parameters

We will study a warm isotropic collisionless plasma with homogeneous initial density distribution. Simulation was carried out via the particle-in-cell method using modified program package PDP1 [13].

The 1D region between two electrodes is simulated. The interelectrode space is filled with a fully ionized hydrogen plasma. The electron beam is injected into the plasma from the left electrode and moves to the right one. Electrodes absorb both plasma and beam particles.

The electron beam is density-modulated:

$$\rho(t) = \rho_0(1 + m \cos \omega t), \quad (1)$$

where  $m$  is the modulation depth. The modulation frequency was selected less than the electron Langmuir plasma frequency  $\omega_p/2\pi = 2.84$  GHz.

Simulation parameters are presented in Table 1.

Simulation was carried out during the time interval of approximately 200 electron plasma periods or 5 ion plasma periods. During this time, the electron beam reached the opposite electrode, and approximately stationary processes were settled (as it was observed in [9, 10]).

Interaction of modes at the modulation frequency and at the frequency of resonant mode differs strongly for various electron beam current densities. The electron beam current density defines the mode of beam-plasma turbulence [14] (see Table 2).

Three simulation series for detailed analysis of these effects were carried out. For the weak turbulence mode, the beam current densities were 0.5, 2, and 4 A/m<sup>2</sup>; for strong turbulence, the value 50 A/m<sup>2</sup> was taken; and, for the superstrong turbulence mode, the beam current density was 150 A/m<sup>2</sup>.

For each mode, the initial modulation depth was varied in the range of 0.01–0.3 with a step of 0.01. The modulation frequency was 2.77 GHz. In comparison with our previous simulation [12], it was moved close to the resonance frequency for the purpose to increase the increment at the modulation frequency (relative bandwidth of the resonant instability is about 10<sup>-5</sup>–10<sup>-6</sup> for our simulation parameters).

### 3. Simulation Results

#### 3.1. Weak turbulence mode

The weak turbulence mode is realized when the energy of beam-excited resonant oscillations is less than the threshold value necessary for the modulation instability [14]:

$$\frac{|E_0^2|}{4\pi n T_e} < 3k_0 \Delta k r_D^2. \tag{2}$$

The energy density satisfying condition (2) corresponds to the electron beam current density in the range (10<sup>-1</sup> ÷ 10<sup>1</sup>) A/m<sup>2</sup>. The value  $j=0.5$  A/m<sup>2</sup> was selected for the further simulation.

The typical space-time distribution of the beam electrons' density and the space dependence of beam electrons' density spectrum are plotted in Fig. 1, *a, b*.

One can see from Fig. 1 that the beam modulation depth grows with the distance from an injector due to the beam-plasma instability. The time period of a signal

in the whole simulation region corresponds to the initial modulation frequency. Only this frequency is observed in the most part of the interelectrode space in the electron beam density perturbation spectrum (Fig. 1, *b*). The spectral component corresponding to the resonant instability appears only near a collector.

Typical dependences of the signal amplitudes at the modulation and resonant frequencies on the coordinate and the initial beam modulation depth, as well as the dependence of the maximal signal amplitude at the modulation frequency on the initial beam modulation depth, are plotted in Fig. 2, *a–c*.

Figure 2, *a* demonstrates that the signal amplitude at the modulation frequency tends to grow with the distance from an injector and the initial modulation depth. On the other hand, there is no evident dependence of the signal amplitude at the resonant frequency on the initial modulation depth. This means that there is no interaction between resonant and non-resonant instabilities in the simulation region, i.e. the linear stage of these instabilities is observed.

Two characteristic regions can be chosen in Fig. 2, *c*.

There is no dependence of the signal maximal amplitude on its initial value for  $m < 0.05$ . In this regime, the initial level of a signal is less than the noise level.

The linear stage of the instability at the modulation frequency in the whole simulation region takes place for  $m > 0.05$ . Consequently, the maximal amplitude of a signal is directly proportional to the initial modulation depth. The signal reaches its maximal value near a collector in this regime.

**Table 1. Selected simulation parameters**

Electron and ion plasma densities	10 <sup>11</sup> cm <sup>-3</sup>
System length	20 cm
Thermal velocity of plasma electrons	6 × 10 <sup>7</sup> cm/s
Thermal velocity of plasma ions	2.33 × 10 <sup>6</sup> cm/s
Velocity of beam electrons	2 × 10 <sup>9</sup> cm/s
Electron beam modulation frequency	2.77 GHz
Electron beam modulation depth	0.01–0.3 with a step of 0.01
Simulation time step	10 <sup>-13</sup> s

**Table 2. Modes of beam-plasma turbulence and appropriate beam current densities**

	Weak turbulence mode	Strong turbulence mode	Superstrong turbulence mode
Order of values of electron beam current density $J$ (A/m <sup>2</sup> )	10 <sup>-1</sup> –10 <sup>1</sup>	10 <sup>1</sup> –10 <sup>2</sup>	> 10 <sup>2</sup>
Used values of electron beam current density $J$ (A/m <sup>2</sup> )	0.5	50	150

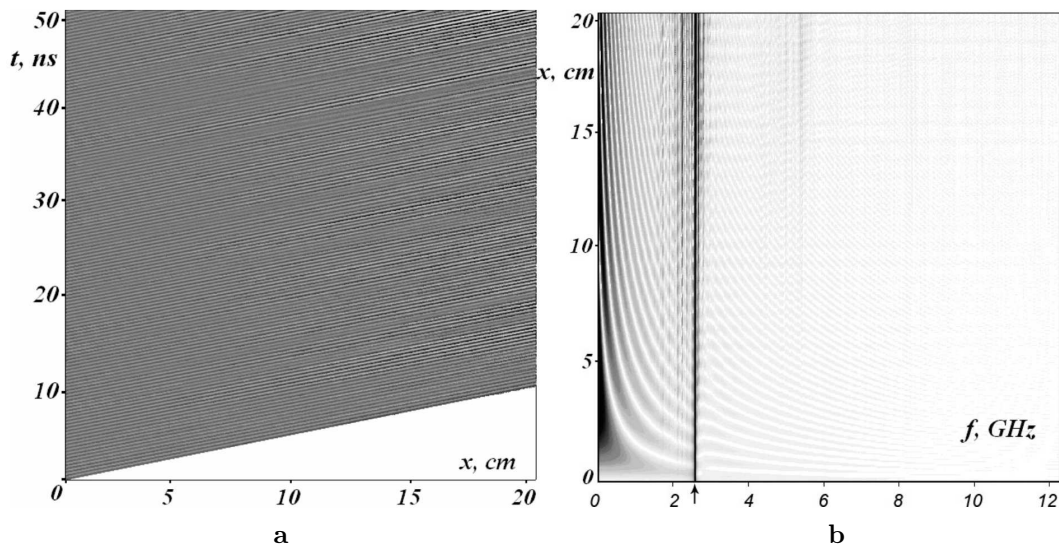


Fig. 1. Space-time distribution of the beam electrons' density (a) and the space dependence of beam electrons' density spectrum (b) for the initial modulation depth  $m = 0.15$  for the weak turbulence mode. The arrow shows a modulation frequency of 2.77 GHz. Dark regions correspond to larger amplitudes

### 3.2. Strong turbulence mode

The strong turbulence mode is realized under conditions contrary to (2). This regime takes place for beam current densities  $10^1$ – $10^2$  A/m<sup>2</sup>. Spontaneous localization of Langmuir oscillations accompanied by the plasma density modulation (modulation instability) is typical of the strong turbulence mode. The modulation instability increment far from its threshold is given by formula [14]

$$\gamma_{Md}(W) = \omega_{pe} \left( \frac{W}{3nT_e} \right)^{1/2} = \omega_{pi} \sqrt{\frac{W}{3nT_e}}, \quad (3)$$

where  $W = E_0^2/4\pi$  is the energy density of the electric field.

The modulation instability increment obtained from the typical time dependence of the relative value of ions' density perturbation ( $2.7 \times 10^6$  s<sup>-1</sup>) is in a satisfactory agreement with the value obtained from (3) –  $3.86 \times 10^6$  s<sup>-1</sup>. So we can conclude that the modulation instability really takes place.

One can see from the comparison of Fig. 1, a and Fig. 3, a that the space-time distribution of beam electrons' density for the strong turbulence mode differs considerably from that of the weak turbulence mode. Light and dark stripes of complicated shapes appear. They correspond to spatial oscillations of the beam modulation depth. The time period of these oscillations corresponds to the beating between the modulation and resonant frequency.

Figure 3, b (fragment of Fig. 3, a) demonstrates a change of the signal time period in the interelectrode region from the initial modulation frequency to the resonant frequency (contrary to Fig. 2, a).

Upper harmonics of the resonant frequency are more significant in the spectrum of electron beam density perturbation (Fig. 3, c). The resonant instability increment grows with the beam current density, so the nonlinear stage of the instability is reached earlier. But, in the electric field strength spectrum, upper harmonics are insignificant, because plasma acts as a high- $Q$  resonator at the Langmuir frequency. Separate spectrum components are widened due to the  $l$ -s decay of a beam-excited Langmuir wave [12].

Note that the dependences presented in Fig. 3 do not change significantly with the variation of the beam modulation depth.

One can see from Fig. 4, a, b that maxima of the resonant signal correspond to minima of a signal at the modulation frequency, and vice versa. There are three characteristic regions differing by the type of interaction of the resonant and non-resonant modes in the range of modulation depth.

For  $m < 0.05$ , the maximum of a non-resonant signal is small relatively to the maximum of the resonant mode. Modes' concurrence takes place, i.e. beam electrons are trapped by the resonant mode; consequently, the growth of the non-resonant mode is suppressed [11]. Qualitatively similar results were obtained in the

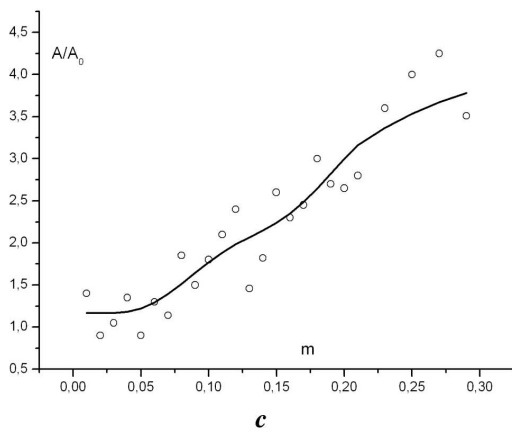
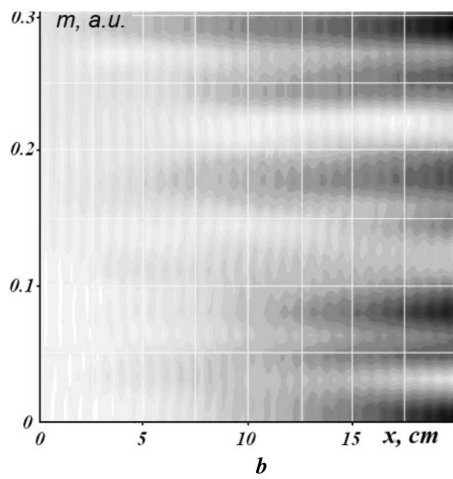
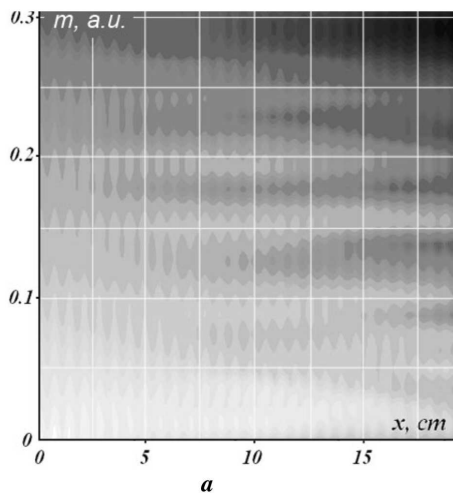


Fig. 2. Dependences of the signal amplitudes at the modulation frequency (a) and the resonant frequency (b) on the coordinate and the initial beam modulation depth and the dependence of the maximal signal amplitude at the modulation frequency on the initial beam modulation depth (c) for the weak turbulence mode

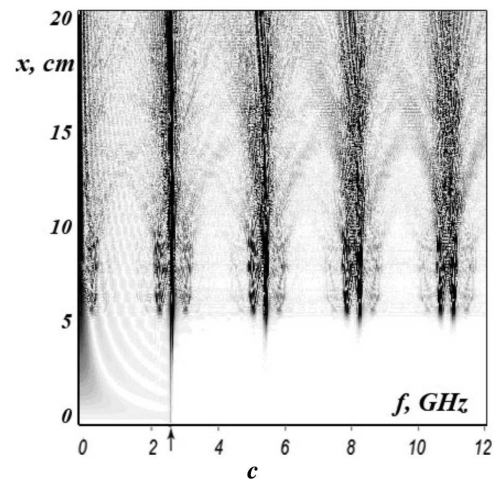
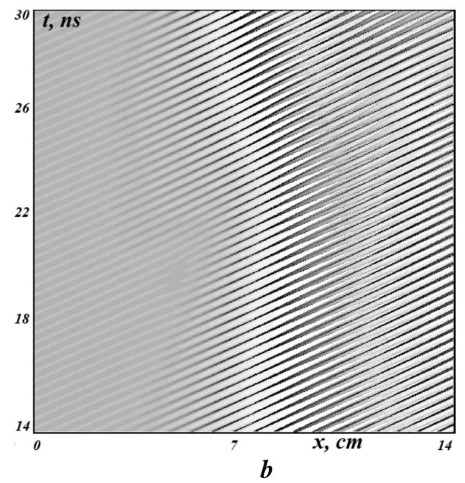
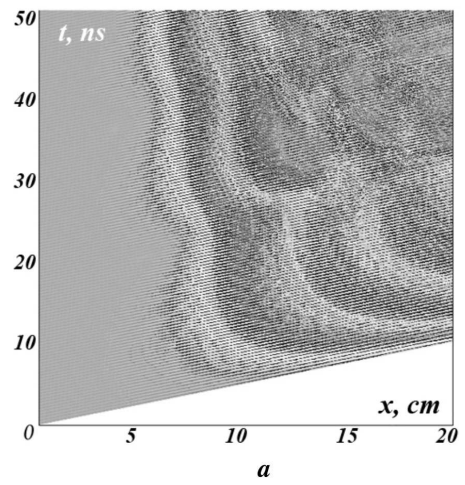


Fig. 3. Space-time distribution of the beam electrons' density (a, b) and the space dependence of beam electrons' density spectrum (c) for the initial modulation depth  $m = 0.1$  for the strong turbulence mode

experiment [9, 10], where only small modulation depths were studied.

For  $m = 0.06 \div 0.07$ , the maximum of a non-resonant signal grows considerably, and its position moves away from an injector. The position of the resonant mode maximum also moves away from an injector and corresponds to a local minimum of the non-resonant signal. In this regime, beam electrons are initially trapped by the non-resonant mode.

For  $m > 0.07$ , the maximum of the non-resonant mode is reached due to the non-linearity of this mode, and its position slowly moves to an injector. This results in the corresponding shift of the resonant mode maximum. Further oscillations of the resonant and non-resonant modes take place in the antiphase.

The comparison of the space-time distributions of the electron beam density for the strong turbulence mode (Fig. 3,*a*) and those under laboratory experiment conditions [12] demonstrates that the laboratory experiment [9,10] corresponds to this regime.

### 3.3. Superstrong turbulence mode

The transition to the superstrong turbulence mode is realized for

$$W_0 \ll \alpha \sqrt{\frac{m}{3M}} k^* r_D 8\pi n T_e, \quad (4)$$

when the inertial interval between the pumping region and the dissipation region in the turbulence spectrum disappears [14]. This condition corresponds to a beam current density of about 100 A/m<sup>2</sup>.

One can see from the comparison of the space-time distributions of beam electrons' density perturbation for the strong and superstrong turbulence modes (Fig. 3,*a* and Fig. 5,*a*) that, in the last regime, wide continuous stripes appear (they start from points A and B). These stripes correspond to the quasiperiodic transillumination of the plasma by an electron beam (instability disappearance). This phenomenon is typical of the superstrong turbulence mode [14]. The dependences presented in Fig. 5 do not change significantly with the variation of the beam modulation depth (similarly to the strong turbulence mode).

The comparison of Figs. 6 and 4 demonstrates the similar character of the interaction of resonant and non-resonant modes for the strong and superstrong turbulence modes. The signal maxima both for resonant and non-resonant modes move to an injector (Fig. 6,*a,b*) due to the growth of the correspondent increments.

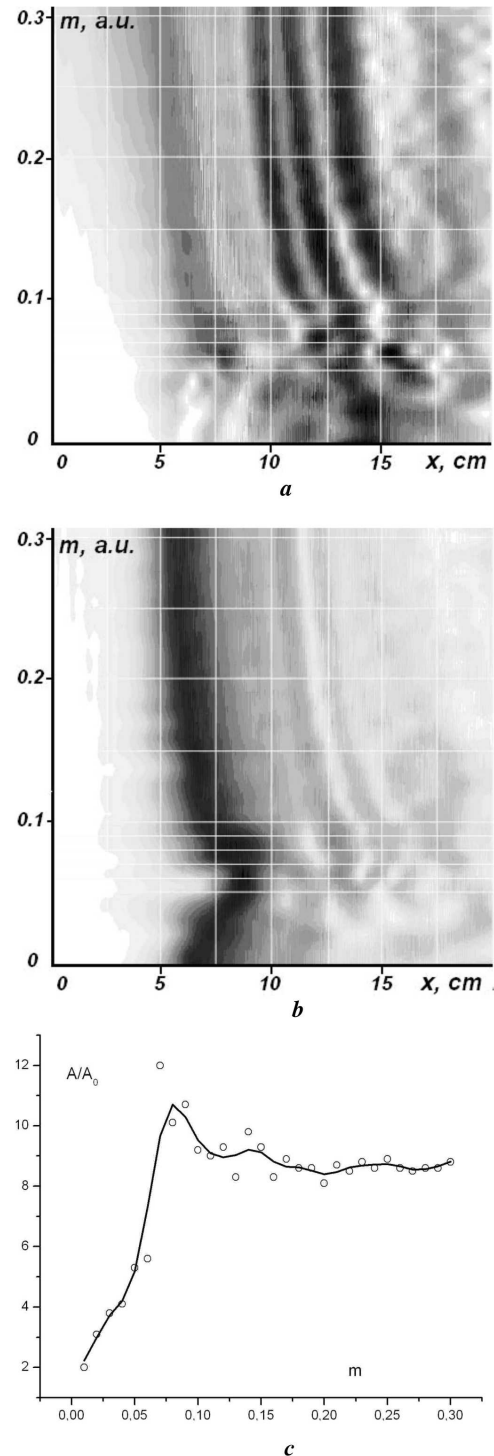


Fig. 4. Dependences of the signal amplitudes at the modulation frequency (*a*) and the resonant frequency (*b*) on the coordinate and the initial beam modulation depth and the dependence of the maximal signal amplitude at the modulation frequency on the initial beam modulation depth (*c*) for the strong turbulence mode

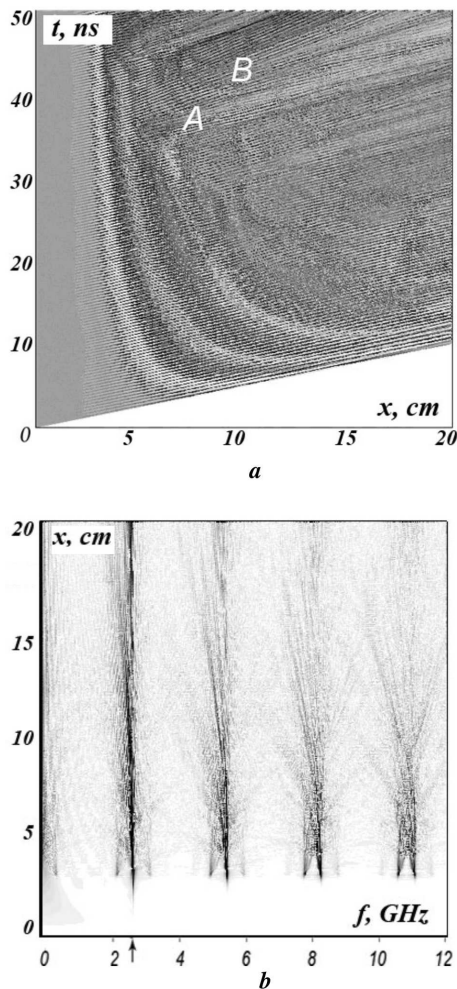


Fig. 5. Space-time distribution of the beam electrons' density (a) and the space dependence of beam electrons' density spectrum (b) for the initial modulation depth  $m = 0.1$  for the superstrong turbulence mode

The value of initial modulation depth, where a local maximum of the dependence  $A/A_0 = f(m)$  is reached for the superstrong turbulence mode, is larger than that for the strong turbulence mode (see Fig. 4,c and Fig. 6,c). This phenomenon can be explained by the different dependences of the resonant and non-resonant increments on the beam current density. We have

$$\gamma_{\text{res}} \sim \left(\frac{n_b}{n}\right)^{1/3}, \quad \gamma_{\text{nonres}} \sim \left(\frac{n_b}{n}\right)^{1/2}, \quad (5)$$

so the increment  $\gamma_{\text{res}}$  grows faster with  $n_b$  than  $\gamma_{\text{nonres}}$  in the region  $n_b/n \ll 1$ . So the initial trapping of beam electrons by a non-resonant mode (regions of the modulation depth of 0.06–0.07 in Fig. 4,c and 0.08–0.12

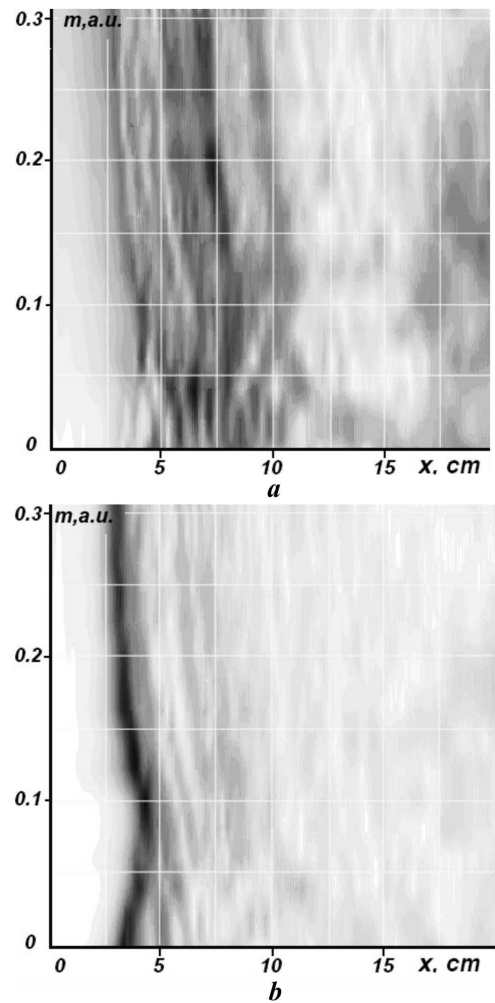


Fig. 6. Dependences of the signal amplitudes at the modulation frequency (a) and the resonant frequency (b) on the coordinate and the initial beam modulation depth and the dependence of the maximal signal amplitude at the modulation frequency on the initial beam modulation depth (c) for the superstrong turbulence mode

in Fig. 6, *c*, respectively) needs a larger initial modulation depth for larger beam current densities.

#### 4. Conclusion

We have determined the ranges of the beam current density corresponding to different modes of beam-plasma turbulence from the simulation and have studied the interaction between resonant and non-resonant (at the modulation frequency) modes.

1. Both resonant and non-resonant increments are very small in the weak turbulence mode. Consequently, both modes do not reach their maxima in the simulation region. Two characteristic regions can be chosen in the range of initial modulation depths  $m$ . There is no dependence of the signal maximal amplitude on its initial value for small  $m$ . In this regime, the initial level of a signal is less than the noise level. The linear stage of the instability at the modulation frequency in the whole simulation region takes place for larger  $m$ . Consequently, the maximal amplitude of a signal is directly proportional to the initial modulation depth.

2. Modulation instability was observed in the strong turbulence mode. Different regimes of the interaction of resonant and non-resonant instabilities (modes' concurrence with the trapping of beam electrons by resonant or non-resonant modes and the non-linear stage of the non-resonant instability) are realized for different values of initial modulation depth.

3. Quasiperiodic transillumination of the plasma by an electron beam was observed for the superstrong turbulence mode, which is typical of this mode. The interaction of resonant and non-resonant modes in this regime is similar to that in the case of the strong turbulence. The value of initial modulation depth, where a local maximum of the dependence  $A(m)$  is reached for the superstrong turbulence mode, is larger than that for the strong turbulence mode. This phenomenon can be explained by the different dependences of resonant and non-resonant increments on the beam current density.

1. A.N. Kondratenko and V.M. Kuklin, *Foundations of Plasma Electronics* (Energoatomizdat, Moscow, 1988) (in Russian).

2. M.V. Kuzelev, A.A. Rukhadze, and P.S. Strelkov, *Plasma Relativistic SHF Electronics* (Izd. MGTU, Moscow, 2002) (in Russian).

3. J. Lavergnat and R. Pellat, *J. Geophys. Res.* **84**, 7223 (1979).

4. M. Starodubtsev and C. Krafft, *J. Plasma Physics* **63**, 285 (2000).

5. I.O. Anisimov and K.I. Lyubich, *Ukr. Fiz. Zh.* **42**, 959 (1997).

6. I.O. Anisimov and K.I. Lyubich, *J. of Plasma Physics* **66**, 157 (2001).

7. I.A. Anisimov, S.M. Levitskii, A.V. Opanasenko, and L.I. Romanyuk, *Zh. Tekhn. Fiz.* **61**, 59 (1991).

8. Ya.B. Fainberg, *Fiz. Plazmy* **26**, 362 (2000).

9. I.O. Anisimov, I.Yu. Kotlyarov, S.M. Levitskii, O.V. Opanasenko, D.B. Palets', and L.I. Romanyuk, *Ukr. Fiz. Zh.* **41**, 164 (1996).

10. I.O. Anisimov, N.O. Boiko, S.V. Dovbakh, D.B. Palets', and L.I. Romanyuk, *Ukr. Fiz. Zh.* **45**, 1318 (2000).

11. I.O. Anisimov, S.V. Dovbakh, S.M. Levitskii, G.V. Lizunov, and O.V. Podladchikova, *Visn. Kyiv. Nats. Univer. Radiofiz. Elektr.*, Iss. 2, 10 (2000).

12. I.O. Anisimov and M.I. Kiyanchuk, *Problems of Atom. Sci. Tekhn. Ser. Plasma Electronics and New Methods of Accel.* **5**, N5, 24 (2006).

13. I.O. Anisimov, D.V. Sasyuk, and T.V. Siversky, in *Abstracts of the Conference "Dynamical System Modeling and Stability Investigation"*, Kyiv, 2003, p. 257.

14. E.V. Mishin, Yu.Ya. Ruzhin, and V.A. Telegin, *Interaction of Electron Beams with Ionospheric Plasma* (Gidrometeoizdat, Leningrad, 1989).

#### ЕВОЛЮЦІЯ МОДУЛЬОВАНОГО ЕЛЕКТРОННОГО ПУЧКА В ПЛАЗМІ У РІЗНИХ РЕЖИМАХ ПЛАЗМОВО-ПУЧКОВОЇ ТУРБУЛЕНТНОСТІ

I.O. Anisimov, M.Й. Кіянчук

Резюме

Досліджено еволюцію модульованого електронного пучка в плазмі у різних режимах плазмово-пучкової турбулентності за допомогою комп'ютерного моделювання методом частинок в комірці. У процесі моделювання було отримано діапазони густини струму пучка, що відповідають кожному з режимів плазмово-пучкової турбулентності. Досліджувалися особливості взаємодії нерезонансної (на частоті модуляції) та резонансної нестійкостей у різних режимах плазмово-пучкової турбулентності. У режимі сильної турбулентності спостерігався розвиток модуляційної нестійкості. У режимі надсильної турбулентності було отримано ефект квазіперіодичного просвітлення плазми для електронного пучка.